Re-entrant metallicity and magnetoresistance induced by Ce for Sr substitution in $SrCoO_{3-\delta}$

2006 J. Phys.: Condens. Matter 18 4305

(http://iopscience.iop.org/0953-8984/18/17/017)

INSTITUTE OF PHYSICS PUBLISHING JOURNAL OF PHYSICS: CONDENSED MATTER

J. Phys.: Condens. Matter **18** (2006) 4305–4314 doi:10.1088/0953-8984/18/17/017

Re-entrant metallicity and magnetoresistance induced by Ce for Sr substitution in $SrCoO_{3-\delta}$

A Maignan, B Raveau, S Hébert[1], V Pralong, V Caignaert and D Pelloquin

Laboratoire CRISMAT, UMR 6508 CNRS ENSICAEN, 6 boulevard Maréchal Juin, 14050 CAEN Cedex 4, France

E-mail: sylvie.hebert@ensicaen.fr

Received 4 October 2005
Published 13 April 2006
Online at stacks.iop.org/JPhysCM/18/4305

Abstract

Cerium for strontium substitution allows an oxygen deficient perovskite $Sr_{1-x}Ce_xCoO_{3-\delta}$ to be stabilized with a cerium solubility limited to $x \leqslant 0.15$ (Trofimenko *et al* 1997 *Solid State Ion.* **100** 183). For these samples, the magnetic properties depend clearly upon the oxygen content: $Sr_{0.9}Ce_{0.1}CoO_{2.74}$ and $Sr_{0.9}Ce_{0.1}CoO_{2.83}$ are weak and strong ferromagnets ($T_C = 160$ K), respectively, the maximum ac-magnetic susceptibility of the latter being larger by two orders of magnitude than that of the former. In contrast to other $Sr_{1-x}L_xCoO_{3-\delta}$ series (L = lanthanide, Y^3 or Th^{4+}), the electrical resistivity (ρ) behaviour does not simply reflect the magnetic behaviour. For $x = 0.10$ the re-entrant ρ feature becomes more pronounced whereas the ferromagnetic fraction and cobalt oxidation state increase. This unexpected behaviour could be related to the Ce^{3+}/Ce^{4+} mixed valency, the 4f localized moment of the Ce^{3+} cations interacting with the conduction electrons through a Kondo-like mechanism. It is also found that the increase of oxygen vacancies favours the appearance of magnetoresistance at low T, reaching -50% at 5 K in 7 T for the $Sr_{0.95}Ce_{0.05}CoO_{2.61}$ sample prepared in a sealed tube.

1. Introduction

The $Sr_{1-x}L_xCoO_{3-\delta}$ oxygen deficient perovskites, where $x < 0.5$ and L is a lanthanide or yttrium, form a large family of compounds with background electronic and magnetic states going from insulating antiferromagnet (AFI) [1–6] to metallic ferromagnet (FM) [7]. For instance, the $Sr_{2/3}Y_{1/3}CoO_{3-\delta}$ compound goes from AFI ($T_N = 290$ K) to FM ($T_C = 225$ K) as its oxygen content varies only from 2.66 to 2.70, i.e. as the cobalt oxidation state increases from 3.00 to 3.08 [7]. This emphasizes that these oxides are just on the verge of a transition

[1] Author to whom any correspondence should be addressed.

which could be related to an orbital ordering of intermediate spin Co^{3+} [7, 8]. However, to reach the FM state, strongly oxidizing conditions are required. Clearly the L^{3+} cation helps in stabilizing the oxygen deficient phase but the cobalt oxidation state v_{Co} depends strongly on its concentration according to the expression $v_{Co} = 4 - x - 2\delta$ (1). At present, from the existing data, it appears that for similar preparation conditions x and δ vary in the opposite way, i.e. the oxygen content decreases as the L^{3+} content increases [2]. If one refers to the $SrCoO_3$ ferromagnetic metal containing pure Co^{4+} [9], the search for new FM compounds in this system is limited by the balance between x and δ. From this viewpoint, the results obtained for the $Sr^{2+}_{1-x}Th^{4+}_{x}CoO_{3-\delta}$ series with $v_{Co} = 4 - 2x - 2\delta$ series are worth mentioning since the as-prepared $Sr_{0.9}Th_{0.1}CoO_{2.79}$ is an FM with $T_C = 200$ K, in which the cobalt cation exhibits an oxidation state of 3.38 [10].

Thus, since tetravalent thorium cations play a different role compared to the trivalent lanthanides or yttrium, the structural and physical properties of the $Sr_{1-x}Ce_xCoO_{3-\delta}$ series have been investigated. In a previous study [11], it was shown that the cerium solubility is very narrow since it is limited to 15%. Nonetheless, the transport properties of $Sr_{1-x}Ce_xCoO_{3-\delta}$ have not been studied yet. According to the fact that the cerium cations could be either trivalent or tetravalent and, second, that the crystalline electric field on the 4f moments of the former may interact with the conduction charge carriers leading to a Kondo-like effect, the study of this electrical transport could be interesting. For instance, a Kondo-like effect was invoked in the case of a perovskite manganite to explain the anomalous behaviour of the resistivity [12]. In the following we report on the magnetic and transport properties of the $Sr_{1-x}Ce_xCoO_{3-\delta}$ series with $0 < x \leqslant 0.15$.

2. Experimental details

The $Sr_{1-x}Ce_xCoO_{3-\delta}$ samples have been prepared by two different routes, allowing different oxidizing conditions to be reached. For the former, the polycrystalline samples were prepared by mixing SrO_2, CeO_2 and Co_3O_4 in stoichiometric proportions according to the '$Sr_{1-x}Ce_xCoO_{3.33}$' nominal compositions ($x < 0.3$). About one gram of each sample in bar form (2 mm × 2 mm × 10 mm) is obtained by pressing the powder and then put in a finger-like alumina crucible, which was finally set in a silica ampoule sealed under primary vacuum. The closed ampoules were heated in 6 h up to 1100 °C and fired for 12 h at this temperature. Finally, the ampoules were quenched in air. In the second method the $SrCO_3$, CeO_2 and Co_3O_4 precursors were mixed in the molar ratios $1 - x{:}x{:}1/3$ according to the '$Sr_{1-x}Ce_xCoO_y$' formulae. After decarbonation at 800 °C in O_2 flow, the powder was pressed into bars, which were heated up to 1200 °C in an oxygen flow and then cooled down at 100 °C h^{-1}. Both preparation routes involve oxygen pressures (1–10 MPa) much smaller than those used to reach the 'O_3' oxygen stoichiometric $SrCoO_3$ perovskite, several GPa [13]. In the case of the closed ampoule, the peroxide decomposition and the possible decomposition of CeO_2 according to the $SrO_2 \leftrightarrow SrO + \frac{1}{2}O_2$ and $2CeO_2 \leftrightarrow Ce_2O_3 + \frac{1}{2}O_2$ equilibria, respectively, create an internal oxygen pressure difficult to quantify. In order to try to homogenize both sample series, all the 'as-prepared' compound ceramics have been post-annealed at 600 °C in $P_{O_2} \sim 10$ MPa. The structural characterizations of the black samples obtained were made by x-ray powder diffraction (XRPD) at room temperature using an Xpert Pro diffractometer with Cu Kα radiation ($20° \leqslant 2\theta \leqslant 120°$, 0.02° step). The XRPD data were refined by the Rietveld method (program Fullprof [14]). Samples for transmission electron microscopy (TEM) were crushed in butanol, and the small crystallites were deposited on a holey carbon film, supported by a copper grid. The electron diffraction (ED) study and the energy dispersive spectroscopy (EDS) analyses were carried out with a JEOL 2011CX electron microscope. The

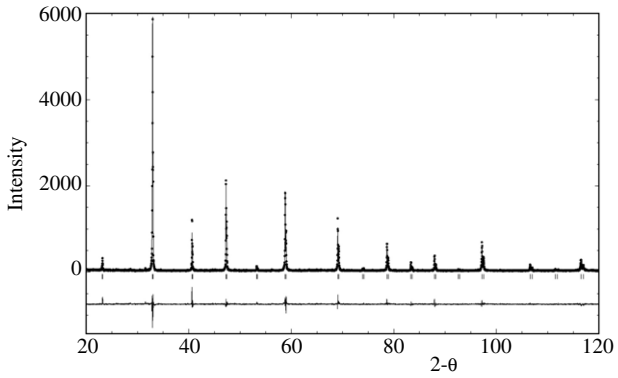

Figure 1. X-ray diffraction pattern of the $Sr_{0.9}Ce_{0.1}CoO_{3-\delta}$ compound prepared in a sealed tube: experimental (points), calculated (lines) and difference (bottom).

oxygen content was determined by iodometric titrations, for which experimental details are given elsewhere [7].

Transport measurements were made by the four-probe technique. Four indium contacts were ultrasonically deposited on the bar and the resistance measurements were made in a physical property measurement system (PPMS, Quantum Design) for 5 K $\leqslant T \leqslant$ 400 K and 0 T $\leqslant \mu_0 H \leqslant$ 9 T. A vibrating sample magnetometer was used to collect the T-dependent magnetization data (1.4 T, zero-field-cooling mode). Ac magnetic susceptibility measurements were made within an applied magnetic field of 10 Oe at a 10^4 Hz frequency.

3. Results

3.1. Structural characterizations

The results of the structural refinements for the $Sr_{1-x}Ce_xCoO_{3-\delta}$ samples prepared in closed ampoules demonstrate the good crystallinity of the samples. The XRPD patterns were refined in the $Pm3m$ space group as shown for the $x = 0.10$ composition in figure 1. The a cubic cell parameter is found to decrease slightly as x increases from $a = 3.850(1)$ Å to $a = 3.846(1)$ Å for $x = 0.05$ to $x = 0.10$, respectively (table 1). Nonetheless, differences in the oxygen contents preclude any discussions about the relationship between x and the cobalt oxidation states. From XRPD refinements, the $x = 0.05$ and $x = 0.10$ compounds are found to be pure but for $x \geqslant 0.15$ some extra peaks belonging to the unreacted CeO_2 oxide were detected in agreement with previous report [11]. In order to check further the purity up to 10% cerium, the $Sr_{0.9}Ce_{0.1}CoO_{3-\delta}$ samples prepared by either O_2 flow or sealed tube have been checked by EDS analyses coupled to ED during TEM studies. First the cation contents of both are similar and in very good agreement with the starting compositions, leading to '$Sr_{0.88}Ce_{0.11}Co_{1.01}$' and '$Sr_{0.86}Ce_{0.11}Co_{1.03}$' for the samples prepared in a closed tube and under oxygen flow, respectively. In the following, the results are thus limited to $x = 0.05$ and $x = 0.10$. Comparison of the a cell parameters (table 1) shows that, for both series, a decreases as the cerium content increases and that the a values for the samples prepared in oxygen flow are smaller than those obtained for closed ampoules.

Considering the EDS analyses which show no significant difference in the cation contents from one series to the other, this strongly suggests that their oxygen content differs. The values of the latter deduced from the titration analyses confirm this point (table 1), since for the same

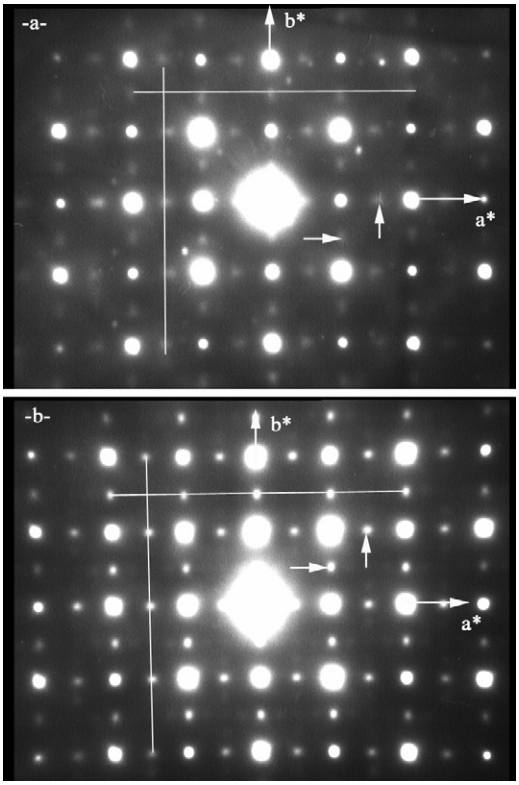

Figure 2. Experimental [001] oriented ED patterns recorded for the as-prepared $x = 0.1$ samples: (a) $Sr_{0.9}Ce_{0.1}CoO_{2.74}$ ('sealed tube') and (b) $Sr_{0.9}Ce_{0.1}CoO_{2.83}$ ('O_2 flow').

Table 1. Oxygen content, cobalt valence (* assuming Ce^{4+} valence) and cell parameter for $Sr_{1-x}Ce_xCoO_{3-\delta}$ ($x = 0.05$ and 0.1) phases.

		Sealed tube synthesis			'O$_2$ synthesis'		
$Sr_{1-x}Ce_xCoO_{3-\delta}$	x	Oxygen content δ	Cobalt valence* ($\pm$0.03)	a (Å)	Oxygen content δ	Cobalt valence* ($\pm$0.03)	a (Å)
	0.05	2.61	3.11	3.850(1)	2.72	3.33	3.846(1)
	0.10	2.74	3.27	3.846(1)	2.83	3.46	3.843(1)

cerium (x) content the oxygen content is higher for the $Sr_{1-x}Ce_xCoO_{3-\delta}$ samples prepared in oxygen flow by about 0.1.

On the structural side, this different oxygen content should affect the superstructure linked to the oxygen vacancy ordering as previously observed in $Sr_{1-x}L_xCoO_{3-\delta}$ [1–5]. To check this, the $Sr_{0.9}Ce_{0.1}CoO_{2.83}$ (oxygen flow) and $Sr_{0.9}Ce_{0.1}CoO_{2.74}$ (closed ampoule) samples were studied by transmission electron microscopy. Besides the presence of numerous 90° domains, a superlattice is systematically observed from ED patterns with a doubling or quadrupling of the c^* axis. A typical $[001]_\infty$ oriented electron diffraction pattern of each sample is shown in figure 2. Clearly, some extra spots are also observed along the a^* and b^* axis (white arrows). This feature has been previously interpreted by considering a supercell ($2a_p \times 2a_p \times 4a_p$) and

the $I4/mmm$ space group[2]. Indeed, in the case of the $Sr_{0.9}Ce_{0.1}CoO_{2.83}$ compound (oxygen flow figure 2(b)), these extra spots imply the doubling of a^* and b^* axes, but in the case of the $Sr_{0.9}Ce_{0.1}CoO_{2.74}$ (closed ampoule) compound they do not lie perfectly at the $(\frac{h}{2}\ 0\ 0)$ and $(0\ \frac{k}{2}\ 0)$ positions (see the white segments in figure 2(a)). In fact, these extra spots reveal a complex microstructure with short-range ordering depending on both the oxygen content and the sample preparation. The $Sr_{0.9}Ce_{0.1}CoO_{3-\delta}$ structure could be described from a modulated $m.a_p$ lattice ($m = 1/q$) or from a superstructure as exemplified by the C-centred lattice ($2\sqrt{2}a_p \times 4a_p \times 2\sqrt{2}a_p$) proposed for $Ln_{0.33}Sr_{0.67}CoO_{3-\delta}$ [5]. However, it is difficult to conclude about this issue due to the small size of the 90° domains, the presence of higher order Laue zone reflections and double diffraction effects. The comparative ED study of these two samples evidences two distinct experimental q vector values which can be correlated to the oxygen content: an incommensurate $q \sim 0.52$ value for $Sr_{0.9}Ce_{0.1}CoO_{2.74}$ and a commensurate $q = 0.5$ value for $Sr_{0.9}Ce_{0.1}CoO_{2.83}$; thus the incommensurability would be related to oxygen deficiency δ such as $\delta \approx 0.25$.

3.2. Physical properties

3.2.1. Evidence for ferromagnetism. The temperature dependence of the magnetization (M) for both series (figure 3) show the large impact of the oxygen content on the magnetic properties of these oxides. The samples prepared under O_2 flow exhibit ferromagnetism with much higher M values at 5 K than those of the samples prepared in sealed tubes. For $x = 0.1$, the maximum magnetization values in 1.45 T are 0.7 μ_B/fu and 0.03 μ_B/fu for the former and the latter, respectively (figure 3(a)). The crucial role of the oxygen content upon the magnetic properties is also confirmed by the measurements made after post-annealing treatments in an O_2 pressure of 15 MPa showing the reinforcement of the ferromagnetism for both series (figures 3(b) and (c)). For the $x = 0.1$ samples, after the post-annealing treatment, the M values at 5 K reach 1.05 μ_B/f.u. and 1.2 μ_B/fu for the samples prepared in O_2 flow and tube, respectively. To discard a possible magnetic field-induced ferromagnetism, ac-χ measurements have been collected before and after the P_{O_2} treatment for the $Sr_{0.9}Ce_{0.1}CoO_{3-\delta}$ sample prepared in the closed ampoule. The $\chi'(T)$ curves show a drastic change in the χ' magnitude from a maximum value $\chi' = 1.4 \times 10^{-4}$ emu g^{-1} at 110 K (figure 4(a)) to $\chi' = 6 \times 10^{-2}$ emu g^{-1} at 160 K (figure 4(b)) prior to and after annealing, respectively. The large value reached for the latter confirms the ferromagnetic nature of $Sr_{0.9}Ce_{0.1}CoO_{2.83}$. It must be also emphasized that for both compounds the paramagnetic temperature obtained by extrapolating the inverse magnetic susceptibility curves is positive, which indicates that ferromagnetic interactions dominate. Also, the ferromagnetism of the P_{O_2} annealed sample is conventional if one refers to $\theta_p \sim T_C$ (figure 4(b)). Finally, the Curie–Weiss fitting of the T linear regime of the inverse magnetic susceptibility (figures 4(a) and (b), right y-axis) leads to effective magnetic moments $\mu_{eff} = 3.2\ \mu_B$/Co and $\mu_{eff} = 3.3\ \mu_B$/Co for the as-prepared and post-annealed samples, respectively. Such values are very close to the values reported for oxygen stoichiometric $La_{1-x}Sr_xCoO_3$ perovskite characterized by x values close to $x \sim 0.20$ [16], i.e. for cobalt oxidation states near 3.20. Thus, the curves corresponding to the oxygen pressure post-annealed samples demonstrate that ferromagnetism is induced in the $Sr_{1-x}Ce_xCoO_{3-\delta}$ phases with $x < 0.15$ in a similar way as for $Sr_{1-x}Th_xCoO_{3-\delta}$ [10]. But smaller T_C values are obtained for the former, as illustrated for the sample $x = 0.1$, 170 K (Ce) against 200 K (Th).

[2] During the submission process of the manuscript, a study of the structure and composition for the $Sr_{1-x}Ce_xCoO_{3-\delta}$ has been published [15]; their structural study by transmission electron microscopy of the ($x = 0.1$, $\delta = 0.2$) composition leads to a different interpretation since they have not considered the existence of a structural modulation.

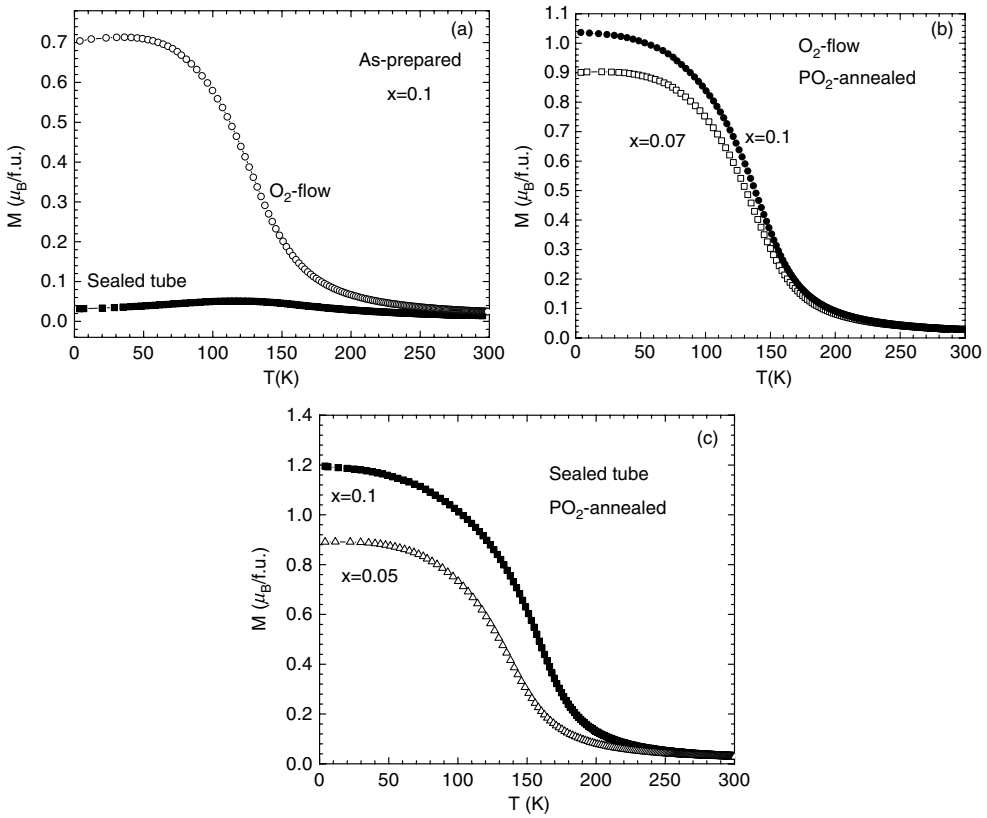

Figure 3. T dependence of the magnetization (M) collected in 1.45 T after a zero-field cooling for the $Sr_{1-x}Ce_xCoO_{3-\delta}$ series. $x = 0.1$ prepared in O_2 flow (O_2) (open circles) or in sealed tubes (ST) (filled squares) (a); samples prepared in O_2 flow and post-annealed under P_{O_2} ($O_2 + P_{O_2}$) (b) and samples prepared in sealed tubes and then P_{O_2} post-annealed (c).

3.2.2. Unusual transport behaviour. The T-dependent normalized resistivity curves $\rho(T)/\rho$ ($T = 390$ K) are given in figure 5 for the samples prepared in sealed tubes (as prepared, figure 5(a) and P_{O_2} annealed, figure 5(b)) or in O_2 flow (P_{O_2} figure 5(c)). As expected from their lack of ferromagnetism, the samples prepared in closed vessels, despite similar ρ values at 390 K ($\rho \sim 1$ mΩ cm), show a strong localization effect developing below $T \sim 100$ K (figure 5(a)). Furthermore, the coefficient $\frac{d\rho}{dT}$ is negative for all T. After the post-annealing treatment responsible for the ferromagnetism creation, the low T resistivity values are strongly decreased (figure 5(b)), the most spectacular result being observed for $Sr_{0.95}Ce_{0.05}CoO_{3-\delta}$, which exhibits a $\frac{d\rho}{dT} > 0$ metallic-like behaviour for $T > 100$ K. However, as one compares the $M(T)$ (figure 5(c)) and $\rho(T)$ curves (figure 5(b)), it is found that the most metallic composition ($x = 0.05$) does not correspond to the strongest ferromagnetism. This result differs from what was reported for the $Sr_{1-x}Th_xCoO_{3-\delta}$ series [10]. Nonetheless, this apparent lack of coincidence between ferromagnetism and metallicity is confirmed by the normalized $\rho(T)$ curves collected after P_{O_2} annealing for the other $Sr_{1-x}Ce_xCoO_{3-\delta}$ series prepared in oxygen flow ($x = 0.07$ and 0.10 in figures 5(c) and 3(b)). It is clear that the most metallic behaviour is found for $x = 0.05$ and $x = 0.07$ compounds but not for $x = 0.1$, despite the larger magnetization of the latter. The effect could reflect the possible interaction between

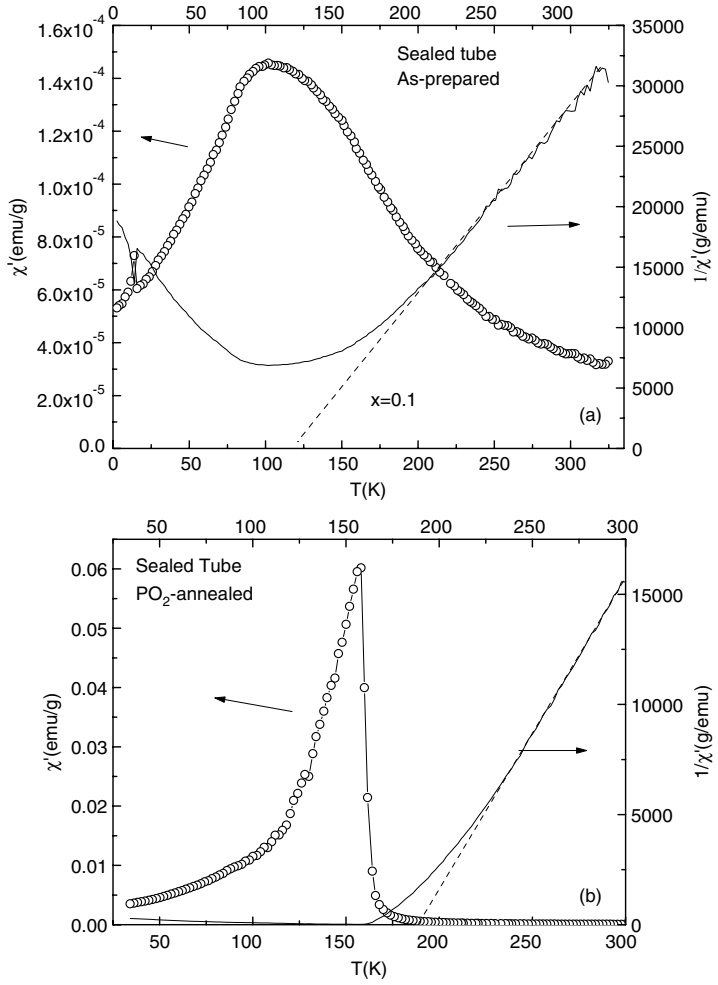

Figure 4. ac-magnetic susceptibility (real part, χ') as a function of T for 'sealed tube' $Sr_{0.9}Ce_{0.1}CoO_{3-\delta}$ samples, as prepared (a) and after P_{O_2} (b). The corresponding inverse magnetic susceptibility curves χ'^{-1} (right y-axis) are also given together with the Curie–Weiss lines (dashed).

the $4f^1$ Ce^{3+} electrons and the 3d cobalt carriers, suggesting that the Ce cations become trivalent for larger x values. Nevertheless, more extrinsic effects due to grain boundaries cannot be ruled out.

3.2.3. Magnetoresistance properties. As shown in figure 6, the $\rho(T)$ data collected upon cooling in 0 and 7 T for the 'O_2' flow $Sr_{0.95}Ce_{0.05}CoO_{3-\delta}$ metallic sample reveal a negative magnetoresistance (MR) starting below about 200 K as T decreases from 390 K. The MR effect has two different origins depending on the T region: a first maximum, at ∼150 K, i.e. near T_C, corresponding to the spin scattering reduction upon external magnetic field application; the second MR kind has a magnitude that increases as T decreases from below T_C down to the lowest T, reaching −7% in 7 T at 5 K. Due to the very different $\rho(T)$ behaviour of the $Sr_{0.9}Ce_{0.1}CoO_{3-\delta}$ samples and, especially, the localization at low T, the MR differs strongly

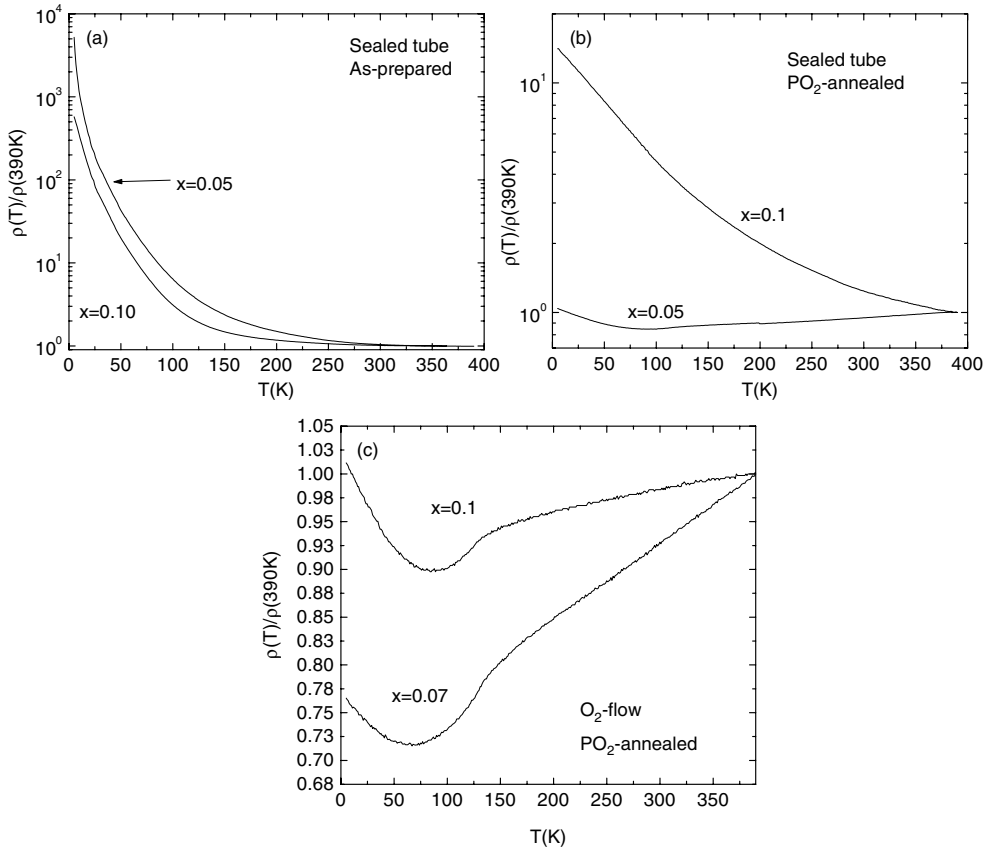

Figure 5. T-dependent normalized resistivity ($\rho/\rho_{390\ \mathrm{K}}$) of the $Sr_{1-x}Ce_xCoO_{3-\delta}$ series. Sealed tubes, as prepared (a) and P_{O_2} annealed (b); samples prepared in O_2 flow and post-annealed in a 15 MPa oxygen pressure (c).

from that of the $x = 0.05$ compound. For all three $Sr_{0.9}Ce_{0.1}CoO_{3-\delta}$ compounds, prepared in O_2 flow (figure 7(a)) or in sealed tubes, before (figure 7(b)) and after (figure 7(c)) P_{O_2} post-annealing, the first MR maximum is suppressed. The MR effect starts to develop below about T_C and its magnitude increases as T decreases down to 5 K. The largest effect, -25% in 7 T, is achieved for the sample prepared in a closed ampoule showing the highest resistivity at low T (figure 7(b)). In fact, an even larger effect is found in the as-prepared $Sr_{0.95}Ce_{0.05}CoO_{3-\delta}$ sample showing a |MR| larger than 50% in 7 T at 5 K (figure 7(d)). This low T contribution to the MR is thus related to the trend towards localization, which becomes more pronounced as the concentration of oxygen vacancies increases.

4. Discussions and concluding remarks

The present similarities between the magnetic properties of $Sr_{0.9}Ce_{0.1}CoO_{2.83}$ and $Sr_{0.9}Th_{0.1}CoO_{2.79}$ [10], with ferromagnetism of $T_C \sim 170$–200 K, suggest that the cerium cations are tetravalent for contents in the solubility region. This result has been also confirmed in an independent study (see footnote 2).

Furthermore, the comparison of the cerium substituted samples, as prepared and post-annealed in oxygen pressure, also shows that the oxygen content plays a crucial role

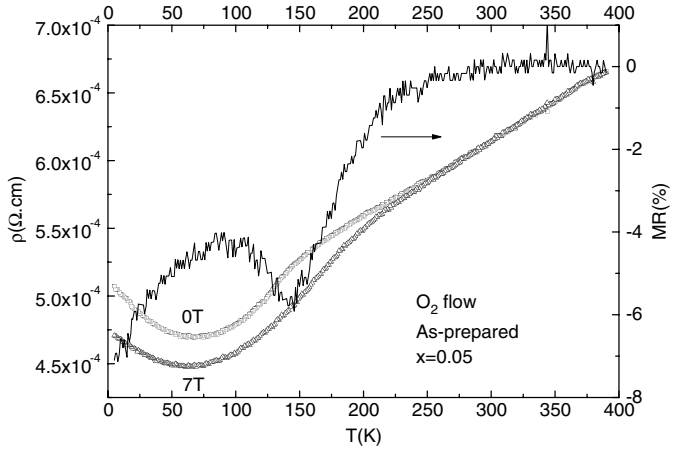

Figure 6. $\rho(T)$ curves of the $Sr_{0.95}Ce_{0.05}CoO_{3-\delta}$ sample prepared in O_2 flow collected upon cooling in 0 and 7 T.

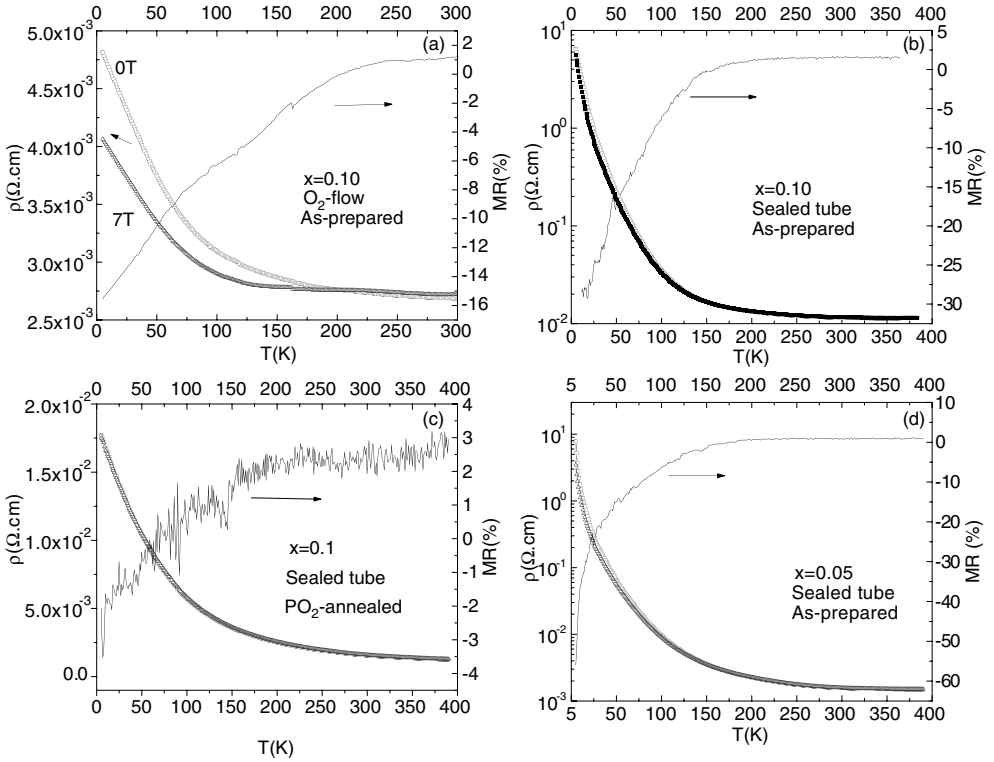

Figure 7. $\rho(T)$ curves (0 and 7 T) of the $Sr_{0.9}Ce_{0.1}CoO_{3-\delta}$ samples. Prepared in O_2 flow (a); prepared in a sealed tube (b) and post-annealed in O_2 pressure (c). The $\rho(T)$ curves of the 'sealed tube' as-prepared $Sr_{0.95}Ce_{0.05}CoO_{3-\delta}$ sample are given for sake of comparison in (d).

in the physical properties: $Sr_{0.9}Ce_{0.1}CoO_{2.74}$ and $Sr_{0.9}Ce_{0.1}CoO_{2.83}$ are weak and strong ferromagnets, respectively.

But the most important difference between cerium cations and lanthanides (or Y^{3+} or Th^{4+}) substituted for strontium lies in the fact that the resistivity (ρ) of the former does not decrease monotonically as the ferromagnetic fraction increases. For the $Sr_{1-x}Ce_xCoO_{3-\delta}$ series it is found that the most metallic composition corresponds to $x = 0.05$ and $\delta \sim 0.28$. In contrast, for higher x values, such as $x = 0.10$, the $\rho(T)$ behaviour becomes much less metallic, as though the magnetization values are enhanced. This Ce induced localization is beneficial to the negative magnetoresistance in the case of the most oxygen deficient compounds since the largest effects are found as the resistivity at low T is the highest.

References

[1] Istomin S Ya, Drozhzhin O A, Svensson G and Antipov E V 2004 *Solid State Sci.* **6** 539
[2] James M, Cassidy D, Goossens D J and Withers R L 2004 *J. Solid State Chem.* **177** 1886
[3] Istomin S Ya, Grins J, Svensson G, Drozhzhin O A, Kozhevnikov V L, Antipov E V and Attfield J P 2003 *Chem. Mater.* **15** 4012
[4] Goossens D J, Wilson K F, James M, Studer A-J and Wang X L 2004 *Phys. Rev.* B **69** 134411
[5] Withers R L, James M and Goossens D J 2003 *J. Solid State Chem.* **174** 198
[6] Goossens D J, Wilson K F and James M 2005 *J. Phys. Chem. Solids* **66** 169
[7] Maignan A, Hébert S, Caignaert V, Pralong V and Pelloquin D 2005 *J. Solid State Chem.* **178** 868
[8] Kobayashi W, Ishiwata S, Terasaki I, Takano M, Grigoraviciute I, Yamauchi H and Karpinnen M 2005 *Phys. Rev.* B **72** 104408
[9] Bezdicka P, Wattiaux A, Grenier J C, Pouchard M and Hagenmuller P 1993 *Z. Anorg. Allg. Chem.* **619** 7
[10] Hébert S, Maignan A, Caignaert V, Pralong V, Pelloquin D and Raveau B 2005 *Solid State Commun.* **134** 815
[11] Trofimenko N E, Paulsen J, Ullmann H and Müller R 1997 *Solid State Ion.* **100** 183
[12] Sundaresan A, Caignaert V, Maignan A, Raveau B and Suard E 1999 *Phys. Rev.* B **60** 533
[13] Kawasaki S, Takano M and Takeda Y 1996 *J. Solid State Chem.* **121** 174
[14] Rodriguez-Carvajal J 1993 *Physica* B **192** 55
[15] James M *et al* 2005 *Mater. Res. Bull.* **40** 1415
[16] Senaris-Rodriguez M A and Goodenough J B 1995 *J. Solid State Chem.* **118** 323